Paper No.
03426

CORROSION 2003

MEASUREMENT OF CORROSION IN SATURATED SOLUTIONS UNDER SALT DEPOSITS USING COUPLED MULTIELECTRODE ARRAY SENSORS

Lietai Yang, Roberto T. Pabalan, Lauren Browning, and Gustavo A. Cragnolino
Center for Nuclear Waste Regulatory Analyses,
San Antonio, TX 78238–5166, U.S.A.

ABSTRACT

The corrosion rates of type 1010 carbon steel, and types 304 and 316 stainless steels in saturated solutions under salt deposits were measured using coupled multielectrode sensors. The measurements were carried out in the presence of the following salts: KCl, NaCl, $NaNO_3$, $MgCl_2$, $NiCl_2$, $FeCl_3$, $FeCl_2$, $CuCl_2$, and an NaCl+$NaNO_3$ mixture.

The results indicate that the corrosiveness of the salts increased in the following order:

$$KCl \sim NaCl \sim NaNO_3 \sim NaCl+NaNO_3 \sim MgCl_2 < NiCl_2 < FeCl_3 < FeCl_2 < CuCl_2$$

for carbon steel, and

$$KCl \sim NaCl \sim MgCl_2 \sim NiCl_2 \sim NaCl+NaNO_3 < FeCl_3 \sim FeCl_2 \sim CuCl_2$$

for type 304 stainless steel.

Some inhibition of corrosion of type 316 stainless steel by $NaNO_3$ was observed in a mixture of NaCl+$NaNO_3$, but not in pure $NaNO_3$ solution.

Key words: galvanically coupled sensor, multiple-electrode sensor, multielectrode, wire beam electrode, localized corrosion, salt deposit corrosion, under salt corrosion

INTRODUCTION

Accumulation of hygroscopic salts on the carbon steel drift support structures, drip shields, and waste packages at the proposed high-level nuclear waste geologic repository at Yucca Mountain, Nevada, may occur due to evaporation of seepage waters and to deposition of aerosol or dust from

ventilation air[1–3]. These hygroscopic salts could sorb moisture from the atmosphere and form brine solutions, which potentially could cause aqueous corrosion of the metals. In addition, the corrosion process could form products that, in combination with these salts, have an even lower deliquescence point that could result in aqueous corrosion at lower relative humidities. Numerous measurements of metal corrosion in aqueous solutions have been reported in the literature, but corrosion measurements in saturated solutions under salt deposits have been rather limited.

In the present work, coupled multielectrode sensors made of carbon and stainless steels were used to measure corrosion rates in saturated solutions under salt deposits. These salts include NaCl, KCl, $MgCl_2$, $NiCl_2$, $NaNO_3$, $FeCl_2$, $FeCl_3$, $CuCl_2$ and an NaCl +$NaNO_3$ mixture. Among these salts, NaCl, KCl, $NaNO_3$, and $MgCl_2$ are likely to form by evaporation of groundwater at Yucca Mountain.[1,2] $FeCl_2$, $FeCl_3$ and $NiCl_2$ may be produced by corrosion of the carbon steel and nickel base alloys used in the drift supports or in the waste package containers in the presence of chlorides.[4,5] Copper is not present in the current design of the engineered repository system, and $CuCl_2$ was selected solely for comparison purpose. Carbon steel is the main material studied here because it will be used in the drift support structure for the proposed repository system[7] and its high corrosion rate in the presence of hygroscopic salts may lead to the formation of corrosion products that are more corrosive than the original salts at low relative humidities.[6] For comparison, many of the measurements also were conducted using sensors made of type 304 and type 316 stainless steels.

EXPERIMENTAL

A drawing of a typical multielectrode sensor used in the experiments is shown in Figure 1. The operating principle and the high-resolution current-measuring system for the coupled electrodes have been described elsewhere.[8-10] In Figure 1, the sensing electrodes are coupled to simulate one piece of a metal and the currents that flow from the anodes (or more anodic electrodes) to the cathodes (or less anodic electrodes) are measured as the corrosion signal. The sensing electrodes of the sensors were made of type 1010 carbon steel (UNS G10100) and types 304 and 316 stainless steels (UNS S30400 and UNS S31600). Each sensor has nine sensing electrodes (of which eight were used in the experiments and one was a spare) cut from 1-mm [0.039 in] diameter wires. The chemical compositions of the carbon steel and the stainless steel wires are listed in Table 1. A total of four carbon steel, four type 304 stainless steel and one type 316 stainless steel sensors were used in this study. The carbon steel and type 304 stainless electrodes were coated with two types of materials (fluoropolymer or epoxy) before being cast in the bulk epoxy. Before each test, the sensing surface of the sensors (the tip of the sensor) were polished with 600-grit paper and cleaned with acetone.

The sensors were inserted through a rubber plug into inverted glass flasks containing the hydrated salts (Figure 2). A small amount of de-ionized water (18 Mohm-cm [7.1 Mohm-in] resistivity) was added to the flask so that the surface of the sensor was fully covered by the saturated solution. The experiments were conducted at room temperature (about 24 °C). The following reagent grade salts were used: KCl, NaCl, $NaNO_3$, $MgCl_2{\cdot}6H_2O$, $NiCl_2{\cdot}6H_2O$, $FeCl_3{\cdot}6H_2O$, $FeCl_2{\cdot}4H_2O$, $CuCl_2{\cdot}2H_2O$, and an NaCl+$NaNO_3$ mixture. The NaCl+$NaNO_3$ mixture was prepared by boiling a solution containing 0.61 mol of NaCl, 1.2 mol of $NaNO_3$, and 100 mL [3.4 fluid ounce] of water until a small amount of free water is left at the bottom.

RESULTS

Figure 3 shows the typical coupling currents from a carbon steel sensor exposed to a wet deposit of NaCl salt during the initial 70 hours of exposure. The anodic coupling current represents the electron flow from a corroding electrode to one or more nearby cathodic electrode(s), and corresponds to the current due to nonuniform corrosion. The highest anodic current can be used to estimate the nonuniform corrosion rate. Microscopic examination of the sensors after the tests indicated that corrosion was nonuniform. As discussed in an earlier paper[8], the current from the most anodic electrode can be approximated by using values derived from statistic parameters, such as the 95th percentile or standard deviation of the currents simultaneously measured from the different electrodes. These derived values can be used to estimate the maximum penetration rate due to nonuniform corrosion. The standard deviation derived from the eight measured currents is also plotted in Figure 3. As shown in this figure, the standard deviation adequately represents the highest anodic current. In most of the measurements in this study, as well as in our previous work,[8,9] the highest anodic current is usually 2 to 4 times the standard deviation.

Figures 4 and 5 show typical plots of the corrosion current densities, represented by 3 times the standard deviation, versus time in the presence of different salts for the carbon and stainless steel sensors. In general, the corrosion current densities are higher during the initial 10 hours of exposure, decaying gradually with increasing time. The high values observed during the initial 10 hours can be attributed to the higher reactivity of the freshly polished electrodes. In addition, the formation and growth of corrosion products on the anodic electrodes during the corrosion process may also cause the decay of the current because they act as a diffusion layer for the reactants and products associated with the corrosion reaction. There were also cases where the coupling current was initially low and increased with time (e.g., the behavior of type 316 stainless steel with KCl and 304 stainless steel with $NiCl_2$ shown in Figure 5). These cases may represent situations where the formation of corrosion products enhanced the corrosiveness of the saturated solutions in equilibrium with the solid salt that is in contact with the corroding electrode.

Figure 5 also shows that some of the measured current densities undergo large fluctuations with time even after the initial 10 hours (e.g., close to one order of magnitude for type 304 stainless steel sensor in the presence of KCl). This behavior may be attributed to the initiation/repassivation processes and the formation of corrosion products on the metal surface that alter the reactive surface area[11] or act as a mass transfer barrier.

Figure 6 shows the corrosion current densities (based on 3 times the standard deviation of the current densities from individual electrodes) from four carbon steel sensors in the presence of different salts. The corrosion current density values and the sensors used for each measurement are listed in Table 2. The data in Figure 6 and Table 2 are values averaged over time after the initial 10-hour period. For repeated tests using the same salts (albeit different sensors), the reproducibility was found to be within ±0.3 in the logarithm scale. No appreciable difference was noted in the results obtained using sensors fabricated with different coating materials.

Figures 7 and 8 show the corrosion current densities (based on 3 times the average values of the standard deviation obtained after 10 hours of exposure) from type 304 and type 316 stainless steel sensors, respectively. Four different sensors were used to obtain the values in Figure 7, whereas only one was used for the data in Figure 8. The various type 304 stainless steel sensors and the values

measured in the presence of different salt deposits are listed in Table 3. No effect of coating materials on the measured current densities was noted.

It was observed that the sensing surface recessed from the epoxy surface for all the electrodes exposed to $CuCl_2$ and for some electrodes exposed to $FeCl_3$. In the case of $CuCl_2$, the deepest and shallowest recesses measured with a micrometer were approximately 1.1 and 0.2 mm [0.043 and 0.0079 in] respectively, after 72 hours of exposure. The shallowest recess was observed on the cathode and is inferred to be caused by general corrosion because there were no net electron flows out of the cathode to the neighboring anodes. The average nonuniform corrosion current density during the 72-hour period is about 0.009 A/cm^2 [0.058 A/in^2], which corresponds to a depth change of 0.8 mm [0.031 in] {97 mm/year at 0.009 A/cm^2 [0.058 A/in^2] for carbon steel[12]}. Assuming that the electrode with the deepest recess was also subjected to the same degree of general corrosion {0.2 mm [0.0079 in]}, the calculated depth is close to the measured depth resulting from nonuniform corrosion {1.1 mm [0.043 in] minus 0.2 mm [0.0079 in] equals 0.9 mm [0.035 in]}. In the case of $FeCl_3$, the deepest recess after 48 hours of exposure was less than 0.1 mm [0.0039 in] (the detection limit of the method). This observation is also consistent with the calculated depth of 0.044 mm [0.001 in] based on the measured nonuniform corrosion current density (about 7×10^{-4} A/cm^2 [4.5×10^{-3} A/in^2] during the 48 hours of exposure).

DISCUSSION

Corrosiveness of Salt Deposits for Carbon Steel

As shown in Figure 5, the measured nonuniform corrosion current density fluctuates considerably with time. Meaningful comparison of corrosiveness of the salt deposits can only be made if the corrosion data are obtained over a long time period. In addition, nonuniform corrosion may be due to the microstructure or composition differences on the metal surface or to differences in the chemical composition of the environment in contact with the metal surface. Therefore, corrosion rates may vary significantly from one location to another (on a microscopic scale). In the extreme case of pitting corrosion, for example, the pit growth rate usually varies considerably from one location to another, giving rise to a distribution of pit depths. As the multielectrode sensors in the present experiment were limited to eight electrodes, each sensor could only simulate a maximum of seven pits (at least one of the eight electrodes has to be a cathode). Thus, the deepest pit of the seven sites may not represent the deepest pit on a metal surface on which hundreds or even thousands of pits may be found. Therefore, the true maximum nonuniform corrosion rate or the highest penetration rate on the metal surface can be determined satisfactorily only when the number of electrodes on a sensor is sufficiently large. Thus, corrosion or penetration rates derived from nonuniform corrosion currents measured in short-term experiments (40 to 72 hours) using an 8-electrode sensor should be considered as preliminary estimates.

Figure 6 shows that the corrosiveness of saturated solutions under the salt deposits on carbon steel increases in the following order:

$$KCl \sim NaCl \sim NaNO_3 \sim NaCl\text{-}NaNO_3 \sim MgCl_2 < NiCl_2 < FeCl_3 < FeCl_2 < CuCl_2 \qquad (1)$$

The corrosion potentials of the carbon steel sensors measured immediately after the tests were –0.536 V_{SCE} (volt versas saturated calomel electrode) and –0.692 V_{SCE} for $NaNO_3$ and KCl, respectively. Both values are close to the redox potential of the couple Fe/Fe^{2+} (E^o= –0.68 V_{SCE}), indicating that the reaction at the electrode, as expected, is dominated by the corrosion of carbon steel:

$$Fe = Fe^{2+} + 2e^{-} \quad (2)$$

In addition, tests repeated using different sensors showed that the nonuniform corrosiveness of the highly oxidizing $FeCl_3$ is lower than that of $FeCl_2$. No explanation can be offered for this observation. The corrosion potentials of the carbon steel sensors measured immediately after the tests were –0.285 V_{SCE} and –0.280 V_{SCE} for $FeCl_3$ and $FeCl_2$, respectively. The two values are close to each other and lie between the redox potentials of the couples Fe^{3+}/Fe^{2+} (E^o=0.53 V_{SCE}) and Fe^{2+}/Fe (E^o= –0.68 V_{SCE}). This observation suggests that $FeCl_3$ was also present in the $FeCl_2$ salt, probably as a result of air oxidation during either storage or measurement, or both. As the corrosion potentials are significantly lower than the redox potential of the couple Fe^{3+}/Fe^{2+}, the measured anodic current, which is used as the sensor signal, is most likely due to the corrosion of the carbon steel electrode, rather than the oxidation of Fe^{2+}. It should be mentioned that the above analyses do not take into account the presence of oxygen because it is present in all the systems studied. In addition, the rate of the oxygen cathodic reaction is usually low and mass-transfer-controlled near the actively corroding sites. However, in the absence of an oxidizing species, as in the case of NaCl or $MgCl_2$ salts, the reduction of oxygen would be the only cathodic reaction at the less actively corroding electrode that could support the nonuniform corrosion reaction occurring at the more actively corroding electrode.

The test results obtained using different sensors (Figure 6 and Table 2) show that $CuCl_2$ is more corrosive than either $FeCl_3$ or $FeCl_2$. From thermodynamics, Fe^{3+} is more oxidizing than Cu^{2+} (Cu^{2+}/Cu^{+}: E^o= –0.088 V_{SCE}; Cu^{2+}/Cu: E^o= 0.096 V_{SCE}; Cu^{+}/Cu: E^o= 0.28 V_{SCE}), and the Fe^{3+}salts should be more corrosive. Post-test observation indicated that copper was deposited on the electrodes, mostly on the cathodic electrodes. The copper deposit was loose and could be removed easily using a soft plastic brush. The corrosion potential of the carbon steel sensor measured immediately after the test in $CuCl_2$ was –0.03 V_{SCE}. Although this value is close to the redox potential of Cu^{2+}/Cu^{+} (E^o= –0.088 V_{SCE}), the measured anodic current, which is used as the sensor signal, is believed to be mainly contributed by the corrosion of the carbon steel electrode, rather than by the oxidation of Cu^{+}. The redox potential of the Fe^{2+}/Fe couple is much lower than that of the Cu^{2+}/Cu^{+} couple (for Fe^{2+}/Fe, E^o= –0.68 V_{SCE}) and the activity of Cu^{+} is expected to be much lower than that of Fe^{2+}. The reason for the high corrosion rate with $CuCl_2$ is not known.

Corrosiveness of Salt Deposits for Stainless Steel

As shown in Figure 7, the corrosiveness of the salts for type 304 stainless steel increases in the following order:

$$KCl \sim NaCl \sim MgCl_2 \sim NiCl_2 \sim NaCl{+}NaNO_3 < FeCl_3 \sim FeCl_2 \sim CuCl_2$$

The measured corrosiveness of $NaNO_3$ +NaCl mixture is comparable to that of the non-oxidizing chlorides. This observation was not expected because $NaNO_3$ usually is considered as a corrosion inhibitor for stainless steels.[13]

The inhibiting effect on the corrosion of type 316 stainless steel by a pure $NaNO_3$ solution is not apparent from the data shown in Figure 8. However, there appears to be some corrosion inhibiting effect of $NaNO_3$ where the solution is a mixture of $NaNO_3$ + NaCl.

The data plotted in Figures 6 through 8 indicate that the nonuniform corrosion currents for the three types of sensors increased in the following order:

Type 316 stainless steel < Type 304 stainless steel < < Type 1010 carbon steel

This order for the stainless steels is consistent with the pitting resistance equivalent numbers of the two types of stainless steels[14].

CONCLUSIONS

The corrosion rates of type 1010 carbon steel and types 304 and 316 stainless steels in saturated solutions under various solid deposits were measured using coupled multielectrode sensors. It was shown that the corrosiveness of the salts increased in the following order:

$$KCl \sim NaCl \sim NaNO_3 \sim NaCl{+}NaNO_3 \sim MgCl_2 < NiCl_2 < FeCl_3 < FeCl_2 < CuCl_2$$

for carbon steel, and

$$KCl \sim NaCl \sim MgCl_2 \sim NiCl_2 \sim NaCl{+}NaNO_3 < FeCl_3 \sim FeCl_2 \sim CuCl_2$$

for type 304 stainless steel.

Some inhibition of corrosion of type 316 stainless steel by $NaNO_3$ is observed in a mixture of $NaCl{+}NaNO_3$, but not in pure $NaNO_3$ solution.

ACKNOWLEDGMENTS

This paper was prepared to document work performed by the Center for Nuclear Waste Regulatory Analyses (CNWRA) for the U.S. Nuclear Regulatory Commission (NRC), Office of Nuclear Material Safety and Safeguards, Division of Waste Management, under Contract No. NRC–02–97–009. The paper is an independent product of the CNWRA and does not necessarily reflect the views or regulatory position of the NRC. The multielectrode sensors used in this study were fabricated under an internal research and development program funded by the Advisory Committee for Research of the Southwest Research Institute. Technical discussions with D.S. Dunn, C.S. Brossia, and N. Sridhar are gratefully appreciated. The assistance of B. Derby and J. Landry with the experiments are acknowledged.

REFERENCES

1. Civilian Radioactive Waste Management System Management and Operating Contractor, “Environment on the Surfaces of the Drip Shield and Waste Package Outer Barrier”, Office of Civilian Radioactive Waste Management System, Management and Operating Contractor, Las Vegas, NV, NL–EBS–MD–000001, Revision 00 ICN 01, 2000.

2. R. T. Pabalan, L. Yang and L. Browning, “Deliquescence Behavior of Multicomponent Salts: Effects on the Drip Shield and Waste Package Chemical Environment at the Proposed Nuclear Waste Repository at Yucca Mountain, Nevada” in Scientific Basis for Nuclear Waste Management XXV, Warrendale, PA: Materials Research Society, Symposium Proceedings Vol. 713, pp. 37-44, 2002.

3. C.S. Brossia, L. Browning, D.S. Dunn. O.C. Moghissi, O. Pensado and L. Yang. "Effect of Environment on the Corrosion of Waste Package and Drip Shield Materials," CNWRA 2001-003, San Antonio, TX: Center for Nuclear Waste Regulatory Analyses, 2001.

4. S. Turgoose, "The nature of surviving iron objects", Conservation of Iron, Nature Maritime Museum Monograph No. 53, National Maritime Museum, Greenwich , pp.1-7, 1982.

5. H.S. Isaacs, J.H. Cho, M.L. Rivers and S.R. Sutton, "In situ X-Ray microprobe study of salt layers during anodic dissolution of stainless steel in chloride solution", J. Electrochem. Soc., Vol. 142, pp.1111-1118, 1995.

6 L. Yang, R.T. Pabalan, L. Browning, and D.S. Dunn, "Corrosion behaviour of carbon steel materials under salt deposits simulated dry repository environments", to be published in Scientific Basis for Nuclear Waste Management XXVI, Warrendale, PA: Materials Research Society, Symposium Proceedings *(MRS meeting, Boston, MA, 2002)*

7. Civilian Radioactive Waste Management System Management and Operating Contractor, "General Corrosion and Localized Corrosion of Waste Package Outer Barrier", Civilian Waste Management System Management and Contractor, Las Vegas, NV, ANL-EBS-MD-000003, Revision 00, 2000.

8. L. Yang, N. Sridhar, O. Pensado, and D. Dunn, "An In-situ Galvanically Coupled Multielectrode Array Sensor for Localized Corrosion", Accepted for publication by Corrosion (November, 2002)

9. L. Yang, and D. Dunn, "Evaluation of Corrosion Inhibitors in Cooling Water Systems Using a Coupled Multielectrode Array Sensor" CORROSION/2002, paper no. 02004, (Houston, TX: NACE International, 2002).

10. L. Yang, and N. Sridhar and G. A. Cragnolino, "Comparison of Localized Corrosion of Fe-Ni-Cr-Mo Alloys in Chloride Solutions Using a Coupled Multielectrode Array Sensor" CORROSION/2002, paper no. 02545, (Houston, TX: NACE International, 2002).

11. N. Sridhar, D.S. Dunn, C.S. Brossia, and G.A. Cragnolino, "Stabilization and Repassivation of Localized Corrosion," in Research Topical Symposium, G.S. Frankel and J.R. Scully (Eds.), (Houston, TX: NACE International, 2001), pp.1-29.

12. ASTM Designation: G102–89 (Reapproved 1999), "Standard practice for calculation of corrosion rates and related information from electrochemical measurements" (1999).

13. Z. Szklarska-Smialowska, Pitting Corrosion of Metals (Houston, TX: NACE International 1986).

14. R.B. Rebak, and P. Crook, "Improved Pitting and Crevice Corrosion Resistance of Nickel and Cobalt Based Alloys," in Proceedings of the Symposium on Critical Factors in Localized Corrosion III, R.G. Kelly, G.S. Frankel, P.M. Natishan and R.C. Newman (Eds.), (Pennington, NJ: Electrochemical Society, 1999), pp.289-302.

Table 1 Chemical compositions (%wt) of the metal wires used in the sensors

Metals	UNS #	Ni	Cr	Fe	Mo	Mn	P	S	C
304 S.S.	S30400	9.5	18.5	Bal	-	<2	-	-	<0.080
316 S.S.	S31600	11	17.7	Bal	3	<2	-	-	<0.12
1010 CS	G10100	-	-	Bal	-	0.31	0.04	0.042	0.08

Note: Bal: Balance

Table 2. Carbon steel sensors and corrosion current densities (based on 3 times standard deviation) measured under different salt deposits

Salts	Sensor ID	I (A/cm^2)	Sensor ID	I (A/cm^2)
KCl	CS#A4	7.0E-06	-	-
NaCl	CS#A2	5.0E-05	-	-
$NaNO_3$	CS#A3	6.0E-06	CS#A4	8.0E-06
NaCl-$NaNO_3$	CS#A2	2.0E-05	-	-
$MgCl_2$.6H2O	CS#A1	2.0E-05	CS#A3	1.5E-05
$NiCl_2$.6H2O	CS#A2	1.0E-04	-	-
$FeCl_3$.6H2O	CS#A4	2.5E-04	CS#A2	7.0E-04
$FeCl_2$.4H2O	CS#A1	4.0E-03	CS#A4	2.6E-03
$CuCl_2$.2H2O	CS#A1	8.5E-03	CS#A3	1.0E-02

Table 3. Type 304 stainless steel sensors and corrosion current densities (3 times standard deviation) measured under different salt deposits

Salts	Sensor ID	I (A/cm^2)	Sensor ID	I (A/cm^2)
KCl	SS#A1	1.5E-05	SS#A5	7.0E-07
NaCl	SS#A3	7.0E-07	SS#A4	1.3E-06
NaCl-NaNO3	SS#A4	2.0E-05	SS#A3	2.0E-06
MgCl2.6H2O	SS#A1	1.0E-06	-	-
NiCl2.6H2O	SS#A3	3.5E-06	-	-
FeCl3.6H2O	SS#A4	3.5E-04	-	-
FeCl2.4H2O	SS#A1	4.0E-04	-	-
CuCl2.2H2O	SS#A1	4.0E-04	-	-

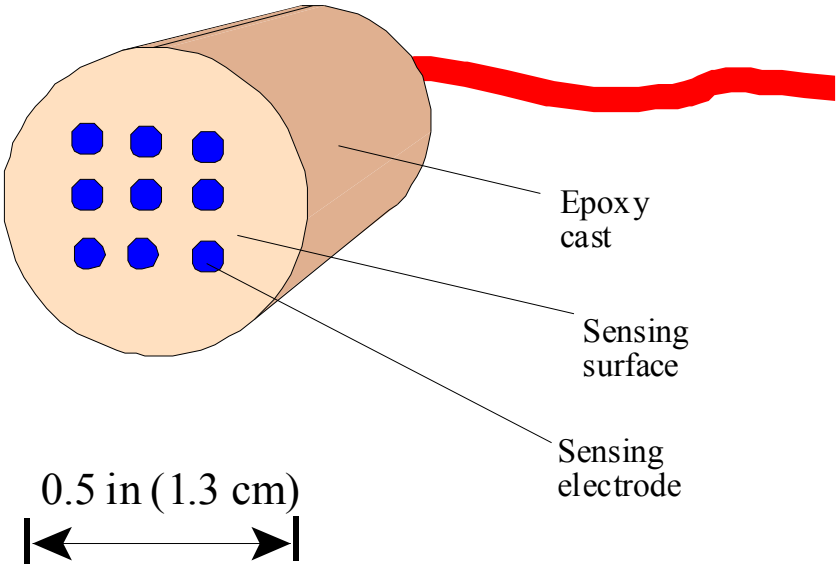

Figure 1 A typical multielectrode sensor used in the experiment

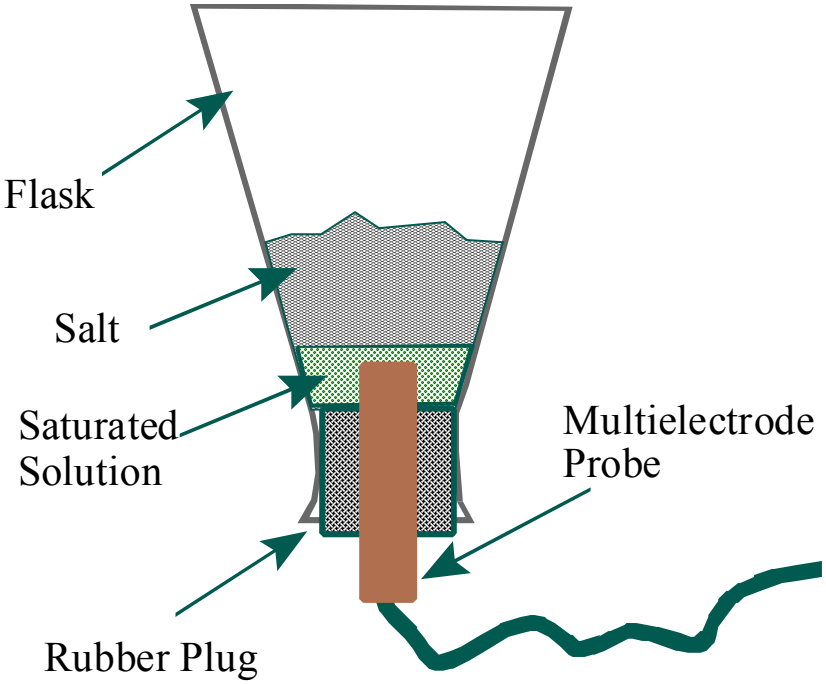

Figure 2 Multielectrode sensor exposed to a saturated solution under a salt deposit

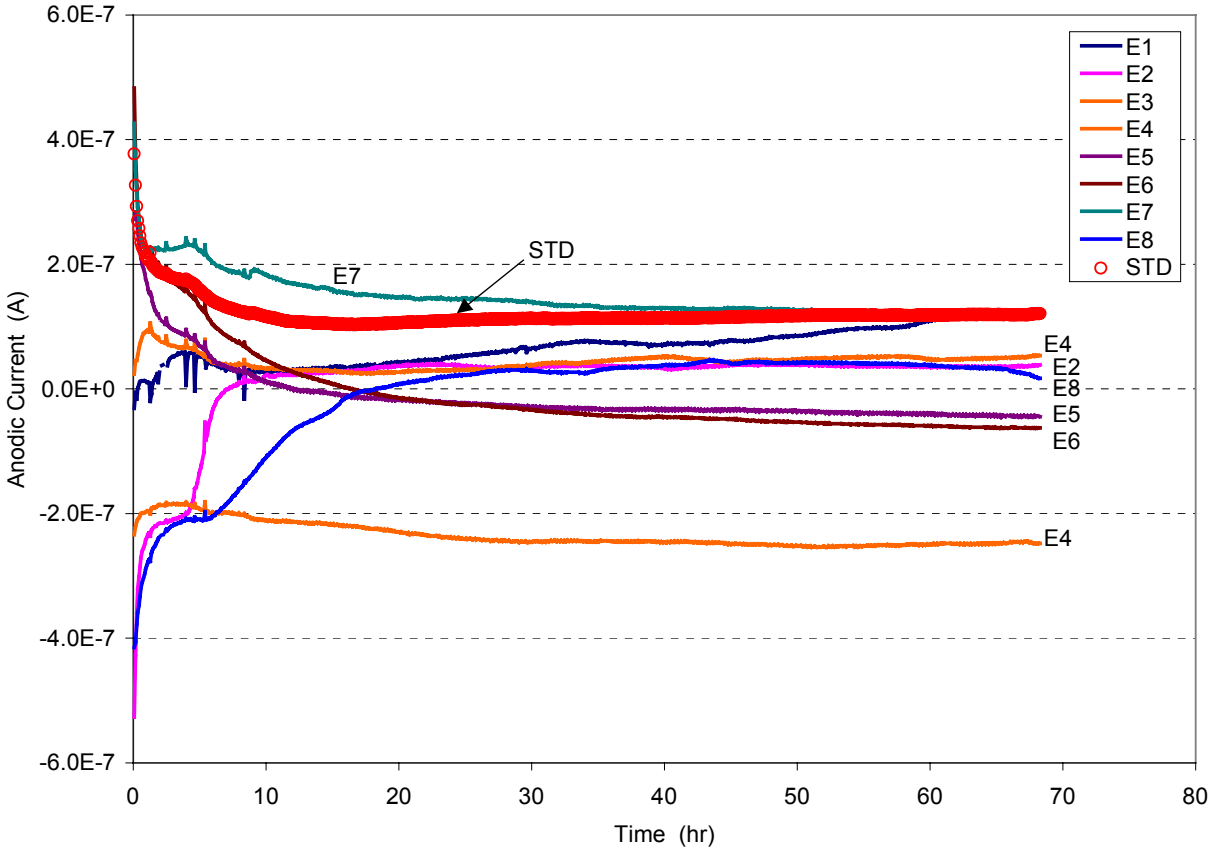

Figure 3 Typical coupling currents from different electrodes of a carbon steel multielectrode sensor exposed to a wet NaCl deposit. Also plotted is the standard deviation (STD) derived from the eight measured currents. E1, E3, … and E8 represent the identification numbers of the electrodes.

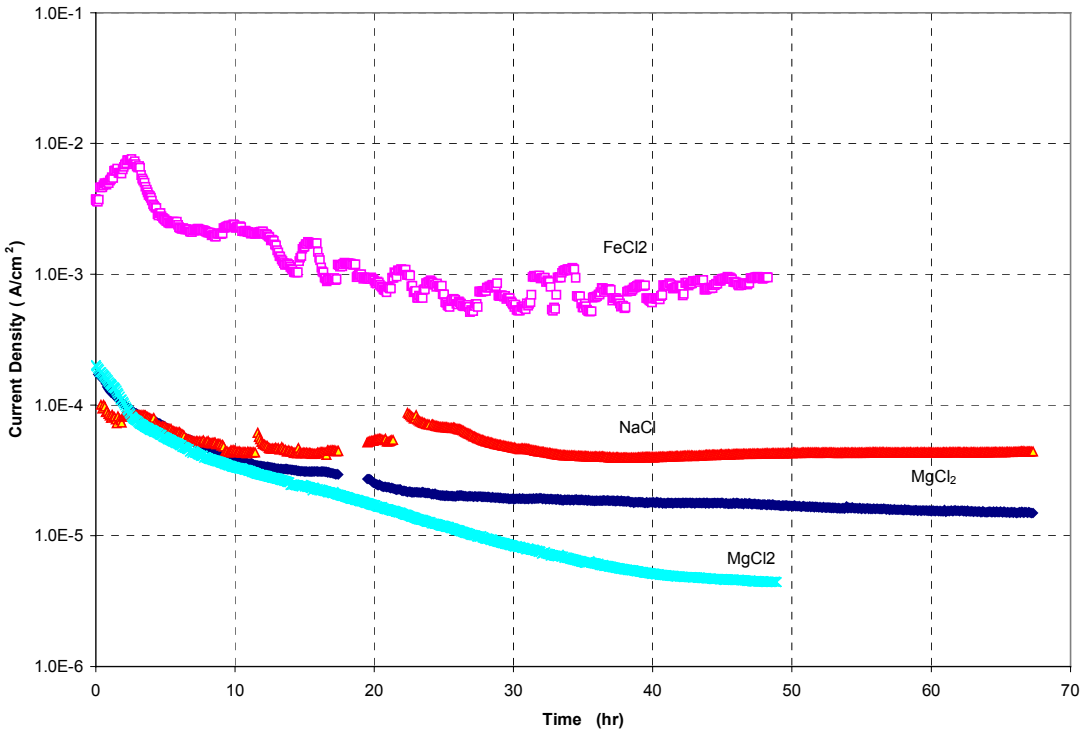

Figure 4 Typical nonuniform corrosion signals for selected carbon steel multielectrode sensors under different salt deposits

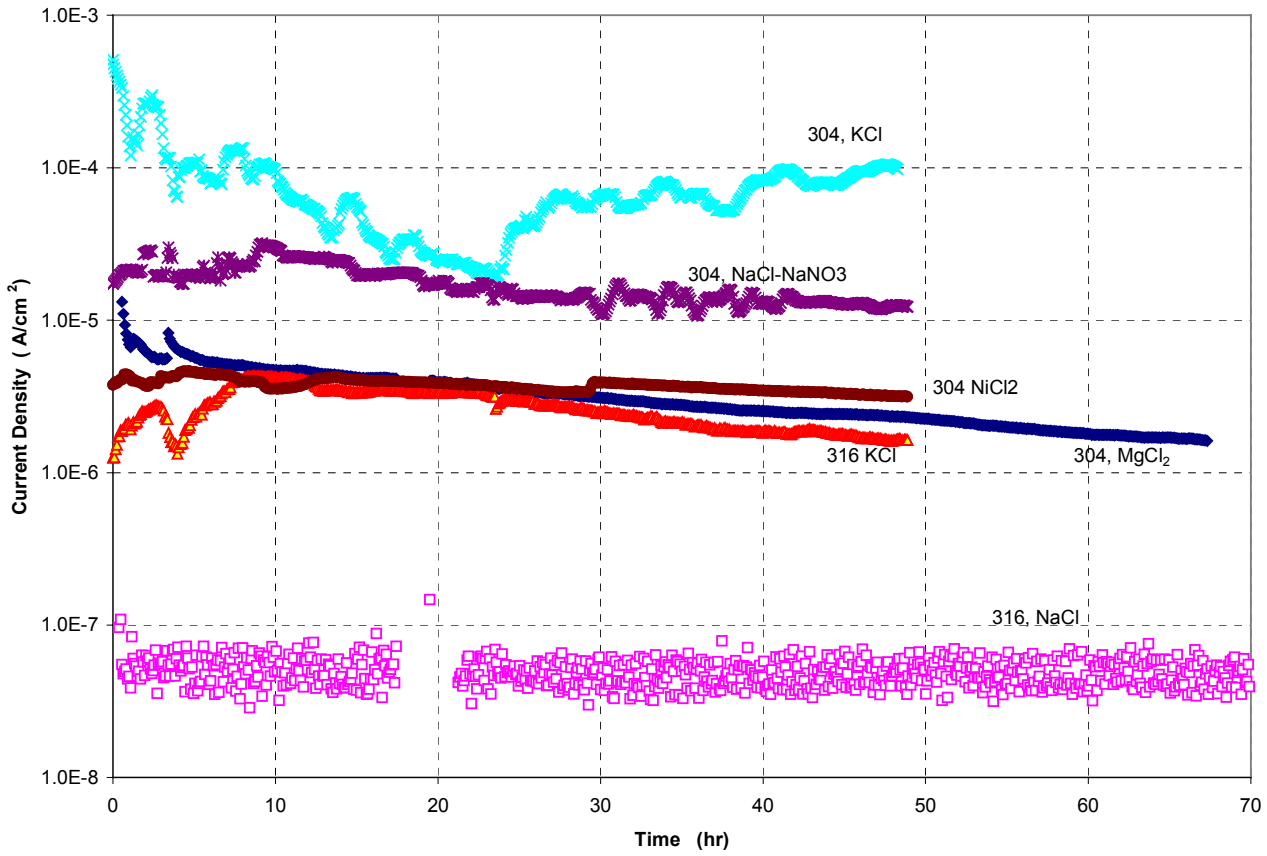

Figure 5 Typical nonuniform corrosion signals for selected stainless steel multielectrode sensors under different salt deposits

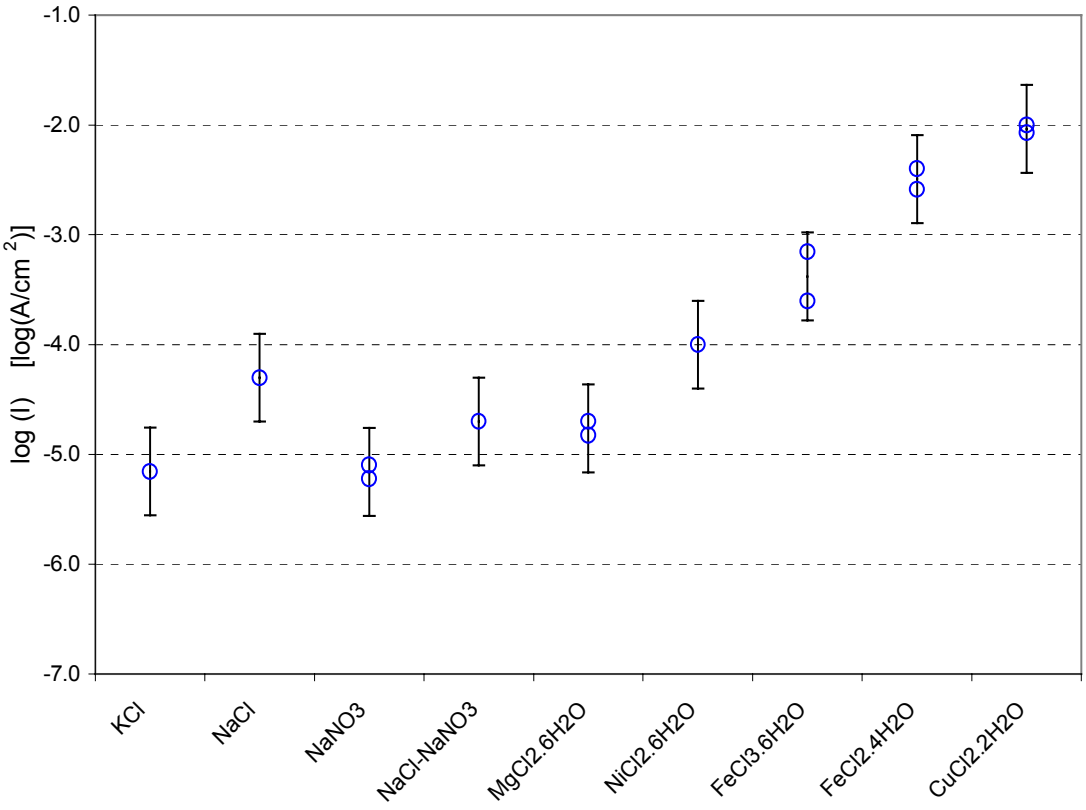

Figure 6 Nonuniform corrosion current densities from carbon steel sensors in the presence of various wet salts

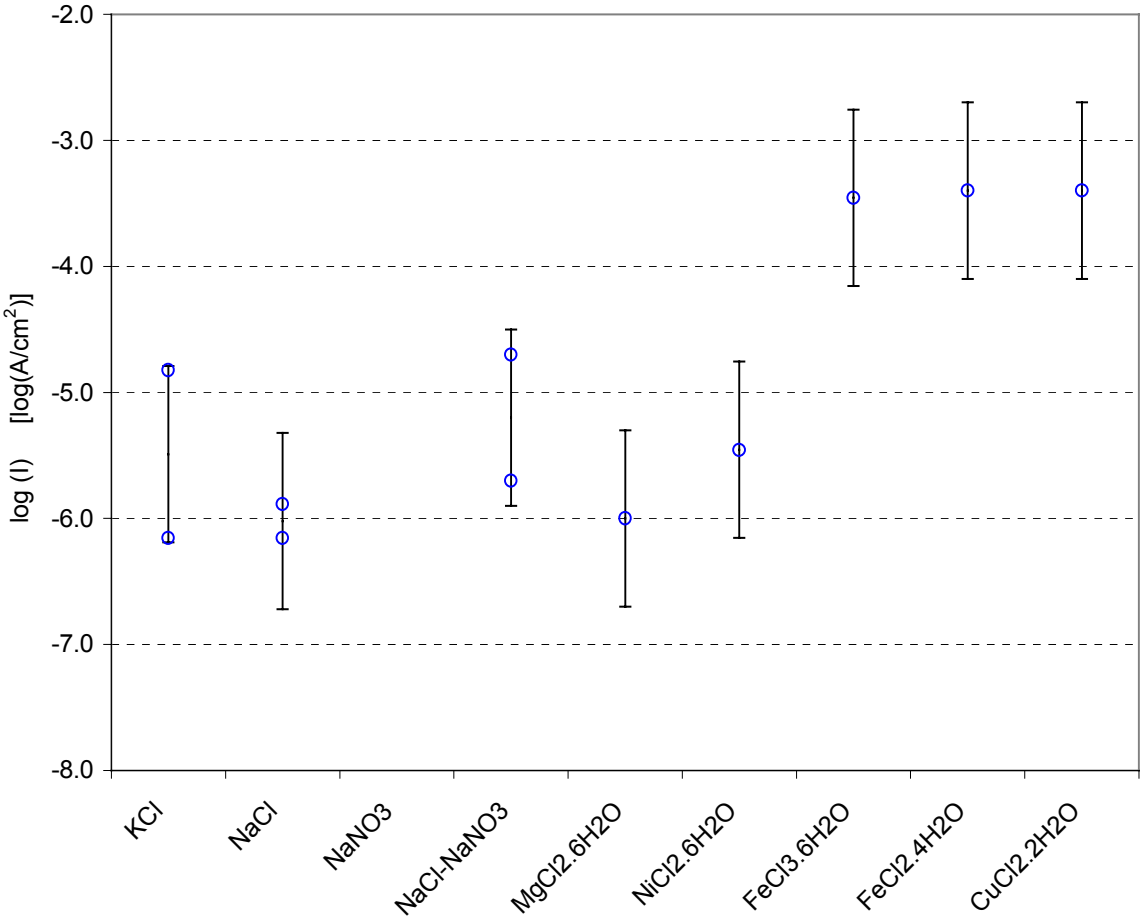

Figure 7 Nonuniform corrosion current densities from type 304 stainless steel sensors in the presence of various wet salts

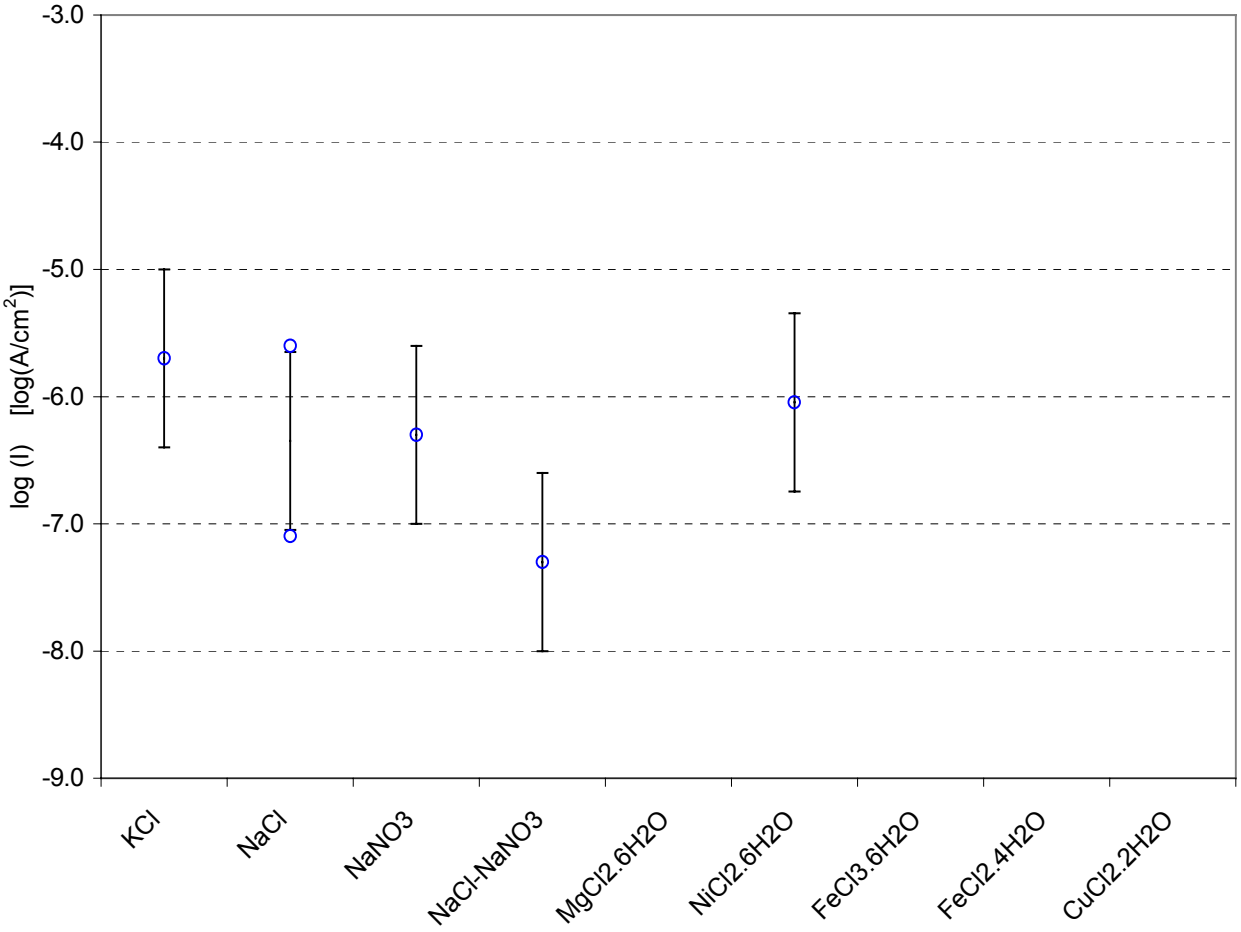

Figure 8 Nonuniform corrosion current densities from a type 316 stainless steel sensor in the presence of various wet salts